Organolanthanide-Catalyzed Hydroamination/Cyclization Reactions of Aminoalkynes. Computational Investigation of Mechanism, Lanthanide Identity, and Substituent Effects for a Very Exothermic C−N Bond-Forming Process

Alessandro Motta,[†] Ignazio L. Fragalà,*[,†] and Tobin J. Marks*[,‡]

Dipartimento di Scienze Chimiche, Università di Catania, and INSTM, UdR Catania, Viale A. Doria 6, 95125 Catania, Italy, and Department of Chemistry, Northwestern University, Evanston, Illinois 60208-3113

Received August 7, 2006

This contribution focuses on organolanthanide-mediated catalytic hydroamination processes and analyzes the exothermic hydroamination/cyclization of a prototypical aminoalkyne, $H_2N(CH_2)_3C{\equiv}CR$, mediated by Cp_2Sm- complexes, using density functional theory. The reaction is found to proceed in two discrete steps, namely, cyclization with concerted Ln−C and C−N bond formation and subsequent Ln−C protonolysis. Dissociation of the cyclized amine then follows to regenerate the active catalyst. Analysis is carried out for (i) insertion of the triple bond moiety into the Sm−N bond via a four-center transition state, (ii) subsequent Sm−C protonolysis by a second substrate molecule, (iii) the effects of other Ln^{+3} ions and aminoalkyne R substituents on the reaction energetics, and (iv) comparison to the analogous, essentially thermoneutral process for aminoalkenes. DFT energetic profiles are computed for the turnover-limiting aminoalkyne C≡C triple bond insertion into the Ln−NH− linkage, and the geometries and stabilities of reactants, intermediates, and products are analyzed. The picture that emerges involves concerted, rate-limiting, exothermic insertion of the alkyne fragment into the Ln−N(amido) bond via a highly organized, seven-membered chairlike cyclic transition state ($\Delta H^{\ddagger}_{calcd} = 4.6$ kcal/mol, $\Delta S^{\ddagger}_{calcd} = -11.9$ eu). The resulting cyclized complex then undergoes exergonic protonolysis to yield an amine−amido complex, the likely resting state of the catalyst. Large rate accelerations effected by smaller lanthanide ions and certain alkyne substituents can be understood in terms of approach distances and charge buildup in the cyclization transition state.

Introduction

Carbon−nitrogen bond-creating processes are of central importance in synthetic chemistry for the preparation of diverse pharmaceuticals, fine chemicals, and materials. For this purpose, atom-efficient hydroamination by catalytic N−H bond addition to unsaturated carbon−carbon multiple bonds represents a challenging, atom-efficient, and highly desirable transformation.[1−3] In comparison to typical middle and late transition metal complexes,[4] those of the lanthanides exhibit unconventional reactivity properties for unsaturated organic substrate conversions and heteroatom transformations.[5] These derive mainly from the appreciable electrophilicity of f-element centers, mechanistic pathways distinctively different from conventional oxidative addition/reductive elimination sequences, nondissociable ancillary ligation, large ionic radii, and very high kinetic

* Corresponding authors. E-mail: lfragala@dipchi.unict.it; t-marks@nothwestern.edu.

[†] Università di Catania.

[‡] Northwestern University.

(1) (a) Funke, F.; Steinbrenner, U.; Boehling, R.; Rudolf, P.; Breuer, K.; Hibst, H. Method and catalysts for producing isopropylamine. PCT Int. Appl., 2003. (b) Steinbrenner, U.; Funke, F.; Boehling, R. Method and device for producing ethylamines and butylamines. PCT Int. Appl., 2003. (c) Boehling, R.; Steinbrenner, U.; Funke, F.; Dier, R. Method for producing amines by means of olefin hydroamination in the presence of unsaturated nitrogen compounds. PCT Int. Appl., 2003. (d) Funke, F.; Steinbrenner, U.; Boehling, R. Method for producing dialkylethylamines from dialkylamines and ethylene in the presence of a sodium dialkylamide hydroamination catalyst. PCT Int. Appl., 2003. (e) Boehling, R.; Steinbrenner, U.; Funke, F. Method for the production of *n*-butyraldehyde and 1-butanol from 1,3-butadiene-containing hydrocarbon streams via hydroamination, isomerization and hydrolysis. PCT Int. Appl., 2003.

(2) For general references, see: (a) March, J. *Advanced Organic Chemistry*, 4th ed.; J. Wiley & Sons: New York, 1992; pp 768−770, and references therein. (b) Brunet, J.-J.; Neibecker, D.; Niedercorn, F. *J. Mol. Catal.* **1989**, *49*, 235−259. (c) Collman, J. P.; Hegedus, L. S.; Norton, J. R.; Finke, R. G. *Principles and Applications of Organotransition Metal Chemistry*; University Science Books: Mill Valley, CA, 1987; Chapters 1, 4, 7, 17. (d) Trost, B. B.; Verhoeven, T. R. In *Comprehensive Organometallic Chemistry*; Wilkinson, G., Stone, F. G. A., Abel, E. W., Eds.; Pergamon Press: Oxford, U.K., 1982; Vol. 8, pp 892−895, and references therein. (e) Gibson, M. S. In *The Chemistry of the Amino Group*; Patai, S., Ed.; Interscience: New York, 1968; pp 61−65.

(3) For leading reviews of amine additions to olefins and alkynes, see: (a) Beller, M.; Tillack, A.; Seayad, J. *Transition Met. Org. Synth.* **2004**, *2*, 403−414. (b) Hegedes, L. S. *Angew. Chem., Int. Ed. Engl.* **1988**, *27*, 1113−1126. (c) Gase, M. B.; Latties, A.; Perie, J. J. *Tetrahedron* **1983**. *39*, 703−731. (d) Backvall, J.-E. *Acc. Chem. Res*. **1983**, *16*, 335−342. (e) Jäger, V.; Viehe, H. G. Houben-Weyl, *Methoden der Organischen Chemie*; Thieme Velag: Stuttgard, Germany, 1977; Vol. 5/2a, pp 713−724. (f) Suminov, S. I.; Kost, A. N. *Russ. Chem. Rev.* **1969**, *38*, 884−899. (g) Chekulaeva, I. A.; Kondraleva, L. V. *Russ. Chem. Rev.* **1965**, *34*, 669−680.

(4) For hydoamination of alkenes and alkynes mediated by middle and late transition metals, see: (a) Brunet, J.-J.; Neibecker, D.; Philippot, K. *Tetrahedron Lett.* **1993**, *34*, 3877−3880. (b) Tamaru, Y.; Hojo, M.; Higashimura, H.; Yoshida, Z.-I. *J. Am. Chem. Soc.* **1988**, *110*, 3994−4002, and references therein. (c) Casalnuovo, A. L.; Calabrese, J. C.; Milstein, D. *J. Am. Chem. Soc.* **1988**, *110*, 6738−6744. (d) Fukuda, Y.; Utimoto, K.; Nozaki, H. *Heterocycles* **1987**, *25*, 297−300. (e) Hegedus, L. S.; Mckearin, J. M. *J. Am. Chem. Soc.* **1982**, *104*, 2444−2451. (f) Pugin, B.; Venanzi, L. M. J. *Organomet. Chem.* **1981**, *214*, 125−133, and references therein. (g) Barluenga, J.; Azar, F.; liz, R.; Rodes, R. *J. Chem. Soc., Perkin Trans.* **1980**, 2732−2737. (h) Coulson, D. R. *Tetrahedron Lett.* **1971**, 429−430. Coulson, D. R. U.S. Pat. 3,758,586, 1973.

10.1021/om060717g CCC: $33.50
Publication on Web 10/12/2006

lability. The facile catalysis of amino alkene hydroamination/cyclization by organolanthanides[5a,6,7] demonstrates that the insertion of olefinic functionalities into Ln−N bonds at bis(cyclopentadienyl)lanthanide(III) centers can be coupled with rapid protonolytic Ln−C cleavage to effect efficient, chemoselective, and regiospecific N−C bond-forming catalysis. Hydroamination/cyclization of primary aminoalkynes formally involves the addition of an N−H bond across a C≡C bond to yield enamines, which subsequently and expectedly undergo tautomerization to the more stable imines[8] at room temperature (eq 1).

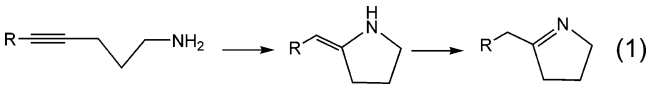

Aminoalkyne-based catalytic processes offer a route to a diverse variety of heterocycles and natural product skeletons (e.g., indolizidines, quinolizidines). Experimental data[9] suggest that hydroamination/cyclization of aminoalkynes consists of three coupled steps, similar to but energetically distinct from those proposed for the hydroamination/cyclization of aminoalkenes: formation of the catalytically active lanthanide amido species via rapid, quantitative proton transfer from the substrate to the hydrocarbyl ligand of the precatalyst[7a,9b] (Scheme 1, step i); turnover-limiting insertion of the alkyne functionality into the Ln−N bond within the stereodirecting framework of the lanthanocene environment (Scheme 1, step ii), followed by subsequent, rapid Ln−C protonolysis of the insertion product to close an efficient catalytic N−C bond-forming cycle (Scheme 1, step iii).

Despite simplistic mechanistic analogies, remarkable differences, both thermodynamic and kinetic/mechanistic, have been established experimentally between aminoalkene and aminoalkyne hydroamination/cyclizations. Under comparable experimental conditions, aminoalkyne hydroamination is both thermodynamically and kinetically favored over aminoalkene hydroamination. Moreover, upon changing the lanthanide in the catalytic center, the two reactions exhibit markedly different and opposite kinetic trends. In the case of aminoalkenes, turnover frequencies decline substantially with decreasing Ln^{+3} ionic radius, while an opposite trend is observed for aminoalkynes.

Scheme 1. Proposed Catalytic Cycle for Organolanthanide-Catalyzed Hydroamination/Cyclization of Aminoalkynes

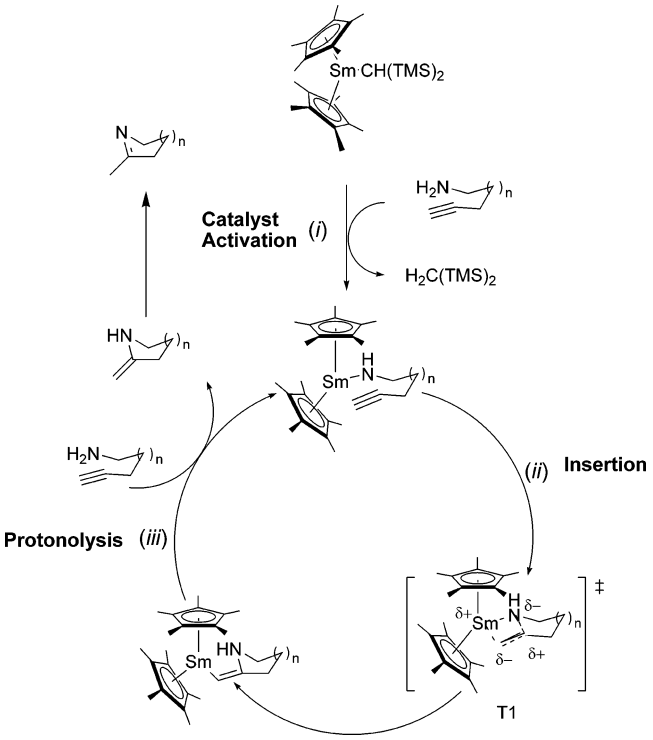

Earlier theoretical studies have analyzed the reaction mechanism for aminoalkene hydroamination/cyclization[10] as well as that for conjugated aminodienes.[11] Similar computational studies have extended the mechanistic analysis to phosphinoalkene hydrophosphination/cyclization.[12] There is, however, no comparable information on aminoalkyne hydroamination/cyclization, which presents an intriguing contrast in view of the markedly greater estimated exothermicity of this process and the very different experimental mechanistic trends vis-à-vis the seemingly analogous aminoalkene process. These considerations motivated an extension of our investigations and a comparison of computational results on aminoalkene hydroamination/cyclization with those on aminoalkynes, to better understand the mechanistic and energetic differences. To allow comparison to our earlier investigations on aminoalkene hydroamination/cyclization,[10] the $Cp_2LnCH(TMS)_2$ catalyst system (Ln = Sm and other lanthanides) and the $NH_2(CH_2)_3C{\equiv}CH$ substrate were selected. These offer a catalytic system for which extensive kinetic/mechanistic data exist and a stereochemically straightforward substrate geometry.

Computational Details

Calculations were performed adopting the closed-shell B3LYP formalism. The effective core potential (ECP) of Stuttgart/Dres-

(5) For general organolanthanide reviews, see: (a) (a) Hong, S.; Marks, T. J. *Acc. Chem. Res.* **2004**, *37*, 673−686. (b) Aspinall, H. C. *Chem. Rev.* **2002**, *102*, 1807−1850. (c) Edelmann, F. T.; Freckmann, D. M. M.; Schumann, H. *Chem. Rev.* **2002**, *102*, 1851−1896. (d) Arndt, S.; Okuda, J. *Chem. Rev.* **2002**, *102*, 1953−1976. (e) Molander, G. A.; Romero, A. C. *Chem. Rev.* **2002**, *102*, 2161−2186. (f) Shibasaki, M.; Yoshikawa, N. *Chem. Rev.* **2002**, *102*, 2187−2210. (g) Inanaga, J.; Furuno, H.; Hayano, T. *Chem. Rev.* **2002**, *102*, 2211−2226. (h) Molander, G. A. *Chemtracts: Org. Chem.* **1998**, *18*, 237−263. (i) Edelmann, F. T. *Top. Curr. Chem.* **1996**, *179*, 247−276. (j) Edelmann, F. T. In *Comprehensive Organometallic Chemistry*; Wilkinson, G., Stone, F. G. A., Abel, E. W., Eds.; Pergamon Press: Oxford, U.K., 1995; Vol. 4, Chapter 2. (k) Schumann, H.; Meese-Marktscheffel, J. A.; Esser, L. *Chem. Rev.* **1995**, *95*, 865−986. (l) Schaverien, C. J. *Adv. Organomet. Chem.* **1994**, *36*, 283−362. (m) Evans, W. J. *Adv. Organomet. Chem.* **1985**, *24*, 131−177. (n) Marks, T. J.; Ernst, R. D. In *Comprehensive Organometallic Chemistry*; Wilkinson, G., Stone, F. G. A., Abel, E. W., Eds.; Pergamon Press: Oxford, U.K., 1982; Chapter 21.

(6) (a) Ryu, J.-S.; Marks, T. J.; McDonald, F. E. *J. Org. Chem.* **2004**, *69*, 1038−1052. (b) Ryu, J.-S.; McDonald, F. E.; Marks, T. J. *Org. Lett.* **2001**, *3*, 3091−3094. (c) Kim, Y. K.; Livinghouse, T.; Bercaw, J. E. *Tetrahedron Lett.* **2001**, *42*, 2933−2935. (d) Molander, G. A.; Dowdy, E. D. *J. Org. Chem.* **1999**, *64*, 6515−6517. (e) Molander, G. A.; Dowdy, E. D. *J. Org. Chem.* **1998**, *63*, 8983−8988.

(7) (a) Gagné, M. R.; Stern, C. L.; Marks, T. J. *J. Am. Chem. Soc.* **1992**, *114*, 275−294. (b) Gagné, M. R.; Marks, T. J. *J. Am. Chem. Soc.* **1989**, *111*, 4108−4109. (c) Giardello, M. A.; Conticello, V. P.; Brard, L.; Gagné M. R.; Marks, T. J. *J. Am. Chem. Soc.* **1994**, *116*, 10241−10254.

(8) Shainyan, B. A.; Mirskova, A. N. *Russ. Chem. Rev.* **1979**, *48*, 107−117, and references therein.

(9) (a) Li, Y.; Marks, T. J. *J. Am. Chem. Soc.* **1998**, *120*, 1757−1771. (b) Li, Y.; Marks, T. J. *J. Am. Chem. Soc.* **1996**, *118*, 9295−9306. (c) Li, Y.; Marks, T. J. *Organometallics* **1996**, *15*, 3370−3372. (d) Li, Y.; Marks, T. J. *J. Am. Chem. Soc.* **1996**, *118*, 707−708. (e) Li, Y.; Fu, P.-F.; Marks, T. J. *Organometallics* **1994**, *13*, 439−440.

(10) Motta, A.; Lanza G.; Fragalà, I. L.; Marks, T. J. *Organometallics* **2004**, *23*, 4097−4104.

(11) Tobisch, S. *J. Am Chem. Soc.* **2005**, *127*, 11979−11988.

(12) Motta, A.; Fragalà, I. L.; Marks, T. J. *Organometallics* **2005**, *24*, 4995−5003.

den,[13,14] which explicitly treats 5s, 5p, 6s, and 5d electrons, was employed for the Sm atom. Calulations on f-element-containing molecules can often be rather difficult due to the presence of an open-shell electron configuration. Thus, calculations explicitly involving 4f electrons are rather limited. This problem has been recently reviewed, and there is good evidence that one is on safe grounds if the 4f electrons are added to the core.[15] This modeling approach finds a parallel in the growing evidence that most reactivity patterns only marginally involve 4f electrons, while 4f electrons must be considered in small-core calculations when spectroscopic properties are desired. It has been shown in many ways that the atomic 4f shells of lanthanide atoms are strongly stabilized and do not contribute significantly to the chemical bonding.[16] However, the f orbital functions are indirectly taken into account by the use of a polarization function added to the lanthanide atom basis set.[17] The standard all-electron 6-31G** basis was used for all remaining atoms.[18] Molecular geometry optimization of stationary points used analytical gradient techniques. The transition state was searched with the synchronous, transit-guided quasi-Newton method.[19] IRC calculations[20] were performed to follow the reaction path through the transition states in both the cyclization and protonolysis steps. Frequency analyses were performed to obtain thermochemical information about the reaction pathways at room temperature. The force constants were determined analytically. All calculations were performed using G98 codes[21] on IBM-SP and Origin 3000 systems.

Results and Discussion

In this section, we discuss the aminoalkyne hydroamination/cyclization catalytic cycle, focusing on both structural changes along the reaction coordinate and energetic aspects, taking into account thermal and entropic effects. Theoretical results will be compared with experiment in regard to these same issues. Moreover, effects arising from other lanthanide catalytic centers and triple-bond α-substituents on the reaction profile are also analyzed.

Catalyst Generation. The geometry of the model precatalyst, $(C_5H_5)_2SmCH(TMS)_2$, is found to adopt a pseudo-trigonal arrangement around the Sm^{3+} ion with the Sm−C(sigma) bond displaced from the $[Cp(centroid)]_2Sm$ plane. This distortion together with the computed bond lengths and angles associated with the TMS groups and the electrophilic Sm center (Sm−C1−Si1, Sm−C1−Si2, Sm−H1, Sm−H2 in Figure 1) indicate substantial deviation from C_s symmetry, consistent with an agostic interaction involving a C1−Si1 bond. This evidence of an agostic interaction is in accordance with XRD and neutron diffraction data on related precatalysts[22] and is a direct consequence of the electron-deficient character of the metal center. Experimental data[9] indicate that the catalyst activation

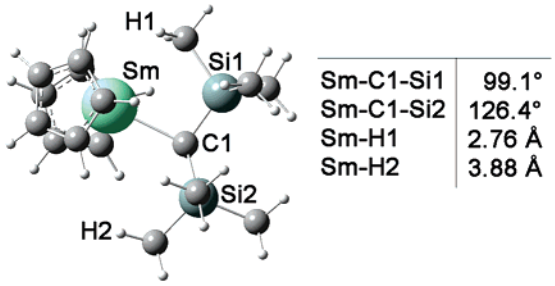

Figure 1. Computed molecular structure of the $(C_5H_5)_2SmCH(TMS)_2$ precatalyst.

process (Scheme 1, step i) is rapid and exothermic, and will not be discussed in detail here since the mechanism involves a protonolysis similar to the second step of the catalytic cycle. This will be analyzed in detail below.

Mechanistic Aspects of the Catalytic Cycle. The activated catalyst can adopt two different conformations (**A** and **B** in Figure 2), depending upon the interaction between the multiple bond and the catalytic core. Conformation **B** is favored on electronic grounds (Figure 3) due to the Sm-coordination of the triple bond. The computational data indicate (Table 1) that cyclization involves progressive approach of the C2 carbon atom toward the N1 center up to ring-closure/N−C bond formation and, as a consequence, synchronous cyclization and reorganization of the Sm coordination environment (Figure 2). During formation of the cyclization product, the Sm−N1 amido bond undergoes elongation to a dative Sm←N1 bond (Sm−N1: 2.569 Å; Table 1). Similarly, the triple bond undergoes progressive saturation to an olefinic double bond (C1−C2: 1.340 Å; Table 1), while the terminal C1 carbon atom evolves to formal sp^2 hyibridization, forming a Sm−hydrocarbyl linkage (Sm−C1: 2.463 Å; Table 1).

IRC calculations on 12 points around the cyclization transition state provide quantitative details on structural changes accompanying the aminoalkyne hydroamination/cyclization process. In particular (Table S1 in Supporting Information), the Sm−N1 and C1−C2 distances increase 0.019 and 0.022 Å, respectively, while the N1−C2 distance decreases 0.208 Å, indicating that the major structural evolution in this step is the ring closure. Thus, the cyclization process involves extensive reorganization of the substrate bonding interactions and consequent energetic stabilization (Figure 3) due to the favorable balance of bond-forming versus bond-breaking processes (vide infra).

In the early stages of the protonolysis step, a new substrate molecule approaches and coordinates to the metal site to form an amine complex (Figure 4). This second substrate unit is modeled here with the simpler methylamine (CH_3NH_2) molecule. In fact, the effects on the protonolysis process arising from the nonproximate unsaturated group represent only a minor energetic effect.[10] Thus, while the energy balance favors, in electronic terms, this coordination mode since the incoming substrate then saturates the electrophilic metal site (Figure 3), entropic factors mitigate against such effects (vide infra).

Protonolytic activation by the CH_3NH_2 substrate involves N2 → C1, H1 exchange with the formation of a C1−H1 bond (Table 2) and shortening of the N2−Sm distance, now characteristic of a Sm−amido bond (Figure 4). As found in the cyclization step, the Sm coordination environment rearranges

(13) Dolg, M.; Stoll, H.; Savin, A.; Preuss, H. *Theor. Chim. Acta* **1989**, *75*, 173−194.
(14) Dolg, M.; Stoll, H.; Preuss, H. *J. Chem. Phys.* **1989**, *90*, 1730−1734.
(15) (a) Eisenstein, O.; Maron, L. *J. Organomet. Chem.* **2002**, *647*, 190−197. (b) Maron, L.; Eisenstein, O. *J. Phys. Chem. A* **2000**, *104*, 7140−7143.
(16) Dolg, M.; Stoll, H. In *Handbook of the Physics and Chemistry of Rare Earths*; Elsevier Science: Amsterdam, 1996; Vol. 22, pp 607−729.
(17) Clark, D. L.; Gordon, J. C.; Hay, P. J.; Martin, R. L.; Poli, R. *Organometallics* **2002**, *21*, 5000−5006.
(18) (a) Hehre, W. J.; Ditchfield, R.; Pople, J. A. *J. Chem. Phys.* **1972** *56*, 2257. (b) Franel, M. M.; Pietro, W. J.; Hehre, W. J.; Binkley, J. S.; Gordon, M. S.; DeFrees, D. J.; Pople, J. A. *J. Chem. Phys.* **1982**, *77*, 3654.
(19) Peng, C.; Schlegel, H. B. *Isr. J. Chem.* **1994**, *33*, 449−454.
(20) (a) Gonzalez, C.; Schlegel, H. B. *J. Chem. Phys.* **1989**, *90*, 2154−2161. (b) Gonzalez, C.; Schlegel, H. B. *J. Phys. Chem.* **1990**, *94*, 5523−5527.
(21) Frisch, M. J.; et al. *GAUSSIAN-98*; Gaussian Inc.: Pittsburgh, PA, 1995.
(22) (a) Jeske, G.; Lauke, H.; Mauermann, H.; Swepston, P. N.; Schuman, H.; Marks, T. J. *J. Am. Chem. Soc.* **1985**, *107*, 8091−8103. (b) Klooster, W. T.; Brammer, L.; Schaverien, C. J.; Budzelaar, P. H. M. *J. Am. Chem. Soc.* **1999**, *121*, 1381−1382.

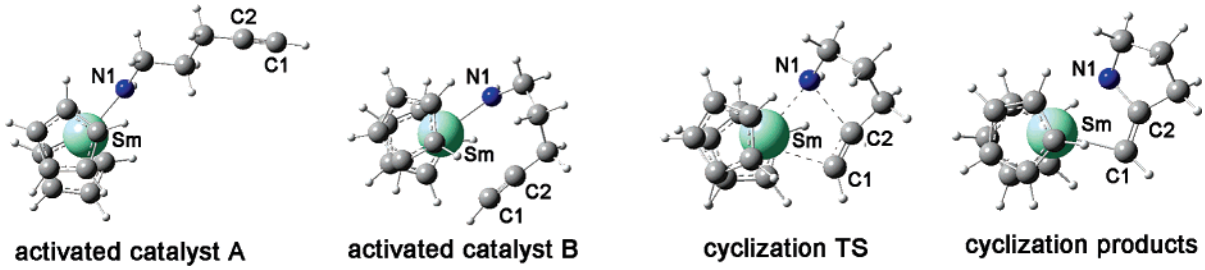

Figure 2. Computed molecular structures involved in the aminoalkyne cyclization step.

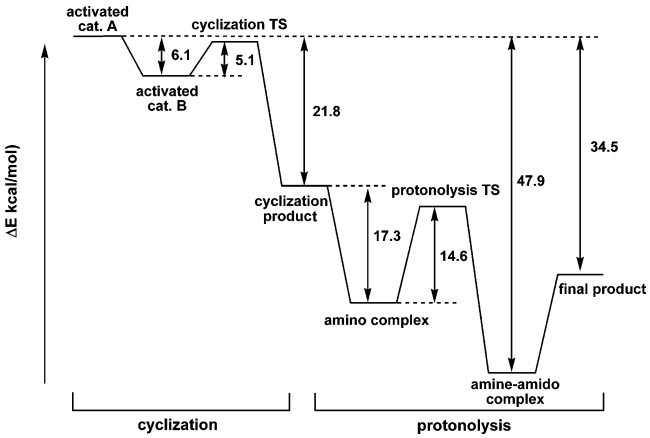

Figure 3. Energetic profile (SCF level) of the aminoalkyne hydroamination/cyclization process.

since an amine−amido complex is formed with scission of the Sm−C1 hydrocarbyl bond (Figure 4). Analysis of the transition state reveals that the atoms involved in this transformation all lie essentially along the same vector (N2−H1−C1 = 163.2°, Table 2).

IRC calculations of 10 points around the protonolysis transition state are in good accord with the dynamics of the process and provide quantitative details on metrical parameter evolution. Thus, the quantitative data (Table S2 in Supporting Information) show that the elongation of the N2−H1 bond (0.486 Å) is comparable to the contraction of the C1−H1 distance (0.484 Å). Moreover, there is a linear correlation between changes associated with the N2−H1 distance and the C1−H1 length, thus providing evidence for a concerted bond-breaking/bond-forming process (Figure 5).

In energetic terms, the above reorganization renders the system more stable due to the favorable balance between bonds broken and formed. The catalytic cycle at this stage releases the product and restores the active catalytic species. The cyclic enamine final product (**C**) further evolves to a more stable (−9.7 kcal/mol) imine tautomer (**D**).

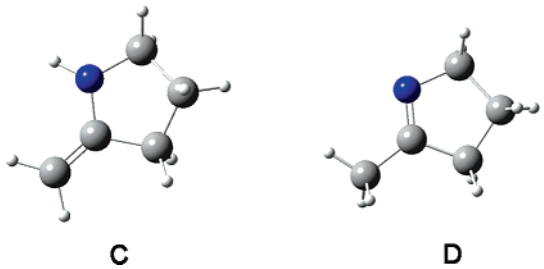

Thermodynamic Aspects of the Catalytic Cycle. To better compare computational results with experiment, effects due to temperature have been accounted for. Solvent effects have been neglected since there is both experimental[7a] and theoretical[12]

Table 1. Bond Length (Å) Involved in the Cyclization Step[a]

	N1−C2	C1−C2	Sm−C1	Sm−N1
activated catalyst **A**	5.020	1.208	7.892	2.243
activated catalyst **B**	3.041	1.218	2.902	2.26
cyclization TS	2.277	1.256	2.589	2.322
cyclization product	1.502	1.340	2.463	2.569

[a] Geometrical parameters refer to Figure 2.

evidence that they are minor. Table 3 summarizes changes in the relevant thermodynamic functions along the reaction profile at 298.15 K. Intriguing differences are evident upon comparing the present results with those for aminoalkene hydroamination/cyclization (Figure 6). Aminoalkyne cyclization is a decidedly exothermic process ($\Delta H = -20.3$ kcal/mol), while the analogous aminoalkene process is essentially thermoneutral ($\Delta H =$ 2.5 kcal/mol). This difference, verified experimentally,[9b] has major consequences upon moving from olefin to alkyne hydroamination. It is therefore of interest to consider the differences between the two processes in terms of the overall energetics associated with bond-breaking and bond-forming. The entire cyclization process, hence the related net enthalpy, involves Sm−C and N−C bond formation and a C−C bond-scission processes. It is reasonable to assume that, to first-order, the bond-forming processes for both aminoalkenes and aminoalkynes are energetically similar. Hence, the more negative enthalpy values found in the case of aminoalkynes are largely independent of the formation of new bonds, and the enthalpy differences must be primarily associated with the C−C bond-breaking processes involving the multiple bonds. Note that the bond-breaking in the aminoalkenes results in a single bond, while in aminoalkynes the triple bond is reduced to an olefinic double bond. Note here that bond enthalpy data[23] show that in the case of olefins this process requires ∼84 kcal/mol, while in the case of alkynes, it requires ∼58 kcal/mol. The latter transformation is therefore far less energetically demanding (∼26 kcal/mol) and accounts well for the greater exothermicity associated with aminoalkyne versus aminoalkene hydroamination. Note also that this C−N bond-forming/cyclization process incurs a sizable entropic cost ($\Delta S = -9.6$ eu) due to greater degree-of-freedom constraints imposed upon evolving from a linear to a cyclic organonitrogen structure (Table 3). In this case, the observed value is similar to that found for aminoalkenes ($\Delta S = -12.9$ eu).

These computational results allow comments on the kinetics of the cyclization step for aminoalkynes. The computed activation enthalpy ($\Delta H^{\ddagger} = 4.6$ kcal/mol) is remarkably smaller than that for aminoalkenes ($\Delta H^{\ddagger} = 11.3$ kcal/mol), and therefore, the greater stability of the products favors more rapid turnover-limiting cyclization, in agreement with experiment.[9a,b] The activation entropy ($\Delta S^{\ddagger} = -11.9$ eu), similar to the ΔS value found for the cyclization products, accounts well for an effective

(23) (a) Chupka, W. A.; Lifshits, C. *J. Chem. Phys.* **1968**, *48*, 1109. (b) Kerr, J. A. *Chem. Rev.* **1966**, *66*, 465.

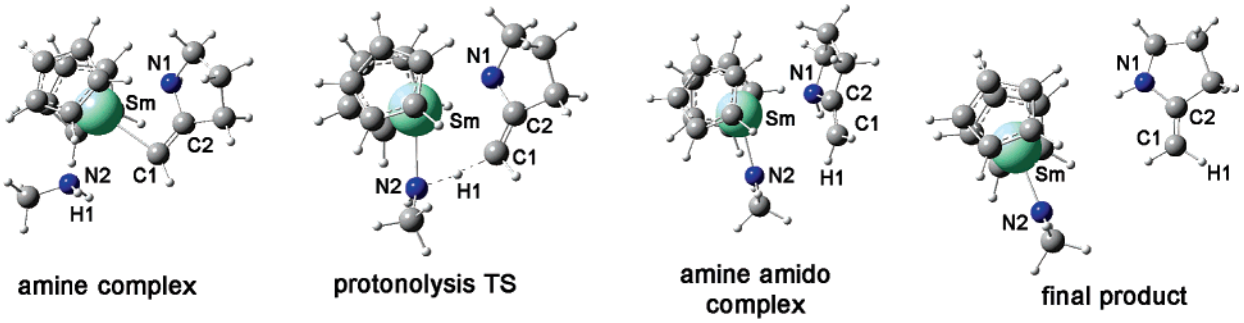

Figure 4. Molecular structures involved in the protonolysis step.

Table 2. Bond Lengths (Å) and Bond Angles (deg) Involved in the Protonolysis Step[a]

	C1−C2	Sm−C1	Sm−N2	N2−H1	C1−H1	N2−H1−C1
amine complex	1.340	2.519	2.639	1.018	2.811	97.9
protonolysis TS	1.339	2.861	2.433	1.331	1.418	163.2
amine−amido complex	1.334	3.968	2.260	4.606	1.084	
final product			2.238			

[a] Geometrical parameters refer to Figure 4.

Table 3. Enthalpy (kcal/mol) and Entropy (eu) Values along the Hydroamination/Cyclization Reaction Profile

	ΔH	ΔS
activated catalyst **A**	0.0	0.0
activated catalyst **B**	−6.4	−8.4
cyclization TS	−1.8	−11.9
cyclization product	−20.3	−9.6
amine complex	−36.2	−51.8
protonolysis TS	−25.3	−55.2
amine−amido complex	−47.0	−49.8
final product	−33.9	−7.6

degrees-of-freedom loss accompanying ring closure, in accord with a well-organized transition state, as again found experimentally. A similar value was computed for the parent aminoalkene process ($\Delta S^{\ddagger} = -14.6$ eu).

The subsequent Sm−C protonolysis step remains exothermic ($\Delta H = -13.6$ kcal/mol) with effects (also structural) similar to those found in the parent aminoalkene hydroamination/cyclization ($\Delta H = -15.5$ kcal/mol) (Figure 7). Comparable entropic changes are also observed (+7.7 eu for olefins versus +2.0 eu for alkynes). As far as kinetic considerations are concerned, theoretical results evidence the lack of any enthalpic energy barrier, with $\Delta H^{\ddagger} = -5$ kcal/mol, for a protonolysis step similar to the case of aminoalkenes ($\Delta H^{\ddagger} = -7.8$ kcal/mol). The negative value clearly reflects the coordination of the second substrate, preceding the protonolysis, which is a strongly exothermic process (−15.9 kcal/mol), that displaces the entire protonolysis energy profile downward (Figure 7).

The formation of the amine−amido complex is similarly responsible for the strongly negative entropic contribution to the protonolysis transition state ($\Delta S^{\ddagger} = -45.6$ eu). The present value, however, is similar to that found for aminoalkenes ($\Delta S^{\ddagger} = -41.3$ eu) and clearly reflects changes in degrees of freedom accompanying bimolecular association to form a single organolanthanide complex (two particles → one). Therefore, the activation barrier involved in this step primarily reflects entropic factors. Thus, the formation of the amine−amido complex is substantially exothermic ($\Delta H = -26.7$ kcal/mol), while the overall enthalpic gain, including elimination of the final product and restoration of the activated catalyst, is −33.9 kcal/mol (Table 3). This value agrees well with experiment. It can be seen that this value is primarily due to the C−N bond-forming cyclization step, even though the protonolysis step provides a sizable contribution.

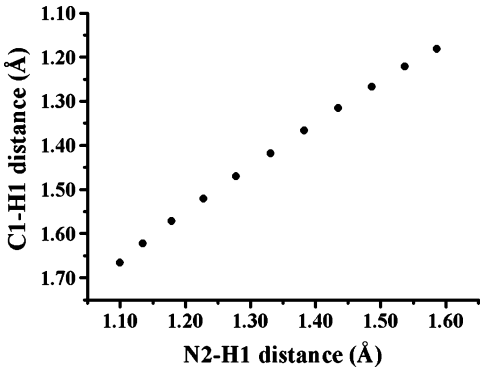

Figure 5. Correlation between the N2−H1 distance and H1−C1 distance in the protonolysis step.

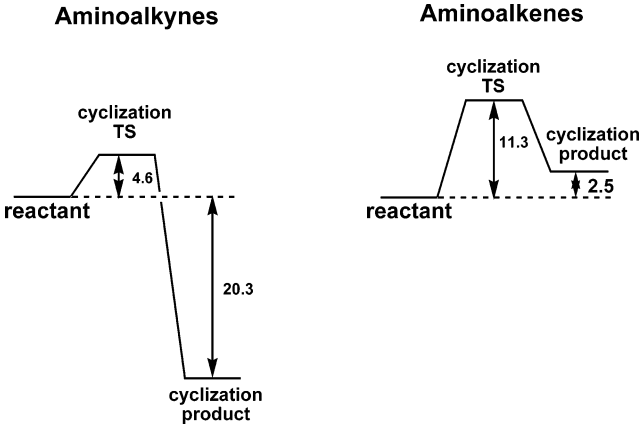

Figure 6. Comparative enthalpic profiles for the cyclization steps in the cases of aminoalkyne and aminoalkene hydroamination/cyclization. Enthalpies in kcal/mol.

The profile of the Gibbs free energy changes along the entire hydroamination/cyclization pathway (Figure 8) reveals several important findings. First, cyclization represents an essentially irreversible exergonic step ($\Delta G = -17.4$ kcal/mol), in agreement with mechanistic observations.[9b] The protonolysis step is similarly spontaneous and essentially irreversible ($\Delta G = -14.1$ kcal/mol), also in agreement with experiment.[9b] That the rate-limiting step is associated with cyclization is in agreement with experimental data.[9b]

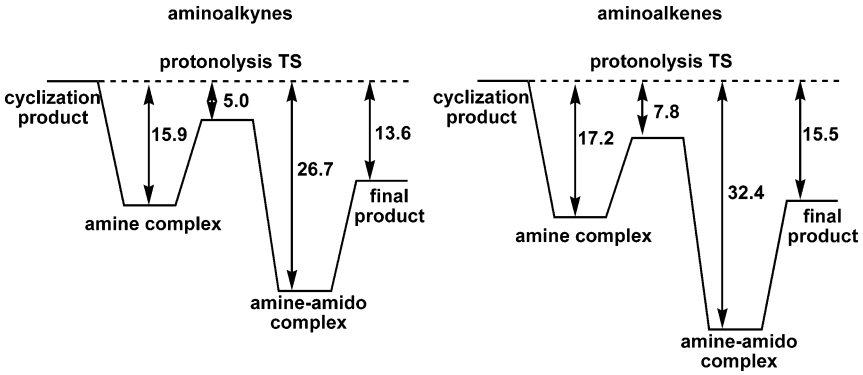

Figure 7. Comparative enthalpic profiles for the protonolysis step in the hydroamination/cyclization of aminoalkynes and aminoalkenes. Enthalpies in kcal/mol.

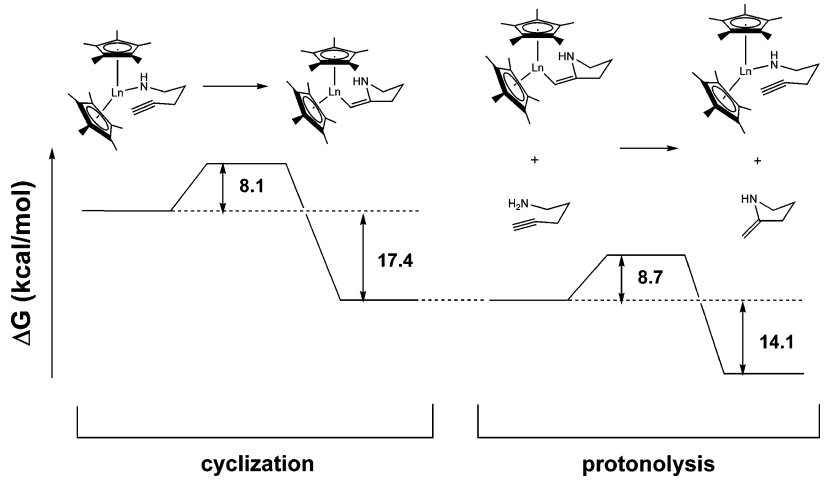

Figure 8. Gibbs free energy (kcal/mol) profile for the hydroamination/cyclization of aminoalkynes.

Table 4. Lanthanide Ion Size Effects on the Cyclization Barrier in Hydroamination/Cyclization of the $H_2N(CH_2)_3C{\equiv}CH$ System

catalyst	ionic radius[a] (Å)	computed $\Delta E^{\ddagger}$ (kcal/mol)	experimental rate[b]
Cp_2La-	1.160	6.1	135
Cp_2Nd-	1.109	5.5	207
Cp_2Sm-	1.079	5.1	580
Cp_2Lu-	0.977	3.9	711

[a] Ionic radii from ref 24. [b] Turnover frequency data (N_t h^{-1} at 21 °C) from ref 9b.

Metal and Substituent Effects on Catalytic Aminoalkyne Hydroamination/Cyclization. In the perspective of substantial experimental evidence that cyclization is the turnover-limiting step, effects due to the Cp_2Ln catalytic center identity have been scrutinized. Thus, the hydroamination/cyclization energetic barriers have been compared for different lanthanide ions, reasonably assuming that thermal and entropic contributions are comparable in all cases. The data in Table 4 show that smaller radii lanthanide catalysts effect the cyclization substantially with smaller activation energies and, hence, greater reaction rates.

These results reproduce well the experimental data (Table 4). In contrast, aminoalkene hydroamination/cyclizations are known to follow an opposite trend, with larger radius lanthanide metals correlating with greater reaction rates. In the latter case, the observed behavior is most likely due to steric hindrance of olefin approach and activation by the catalytic center. In the case of alkynes, steric effects do not appear to be of great relevance due to the lesser encumberance associated with the triple bond. The quantitative reasons underlying this trend can be understood by monitoring distance changes associated with the relevant bonds. Thus, the N1−C2 bond distance changes that accompany cyclization (Figure 2) represent the most reasonable indices of the kinetic behavior (Table 5).

Table 5. N1−C2 Bond Distances (Å) along the Cyclization Coordinate with Varying Lanthanide Catalyst Size[a]

	La	Nd	Sm	Lu
activated catalyst **B**	3.115	3.074	3.041	2.963
cyclization TS	2.283	2.284	2.277	2.302
cyclization product	1.500	1.502	1.502	1.504

[a] Labeling refers to Figure 2.

Importantly, these lengths remain almost constant both in the cyclization products (∼1.50 Å) and in the transition states (2.28−2.30 Å) for all catalysts presently considered. In contrast, large differences are observed in the activated catalysts (Table 5). The data in Table 5 unequivocally indicate that the smaller lanthanide centers facilitate closer N1···C2 approach. That is, the smaller the lanthanide ion, the smaller the structural/energetic reorganization required in the cyclization step and, hence, the smaller the energetic demands.[25]

Finally, effects of the R substituent on the cyclization reaction kinetics have been evaluated (eq 2). Table 6 shows that the

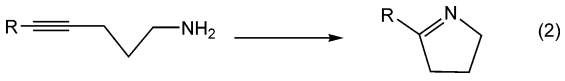

(2)

calculated activation barriers are rather sensitive to the identity of the alkyne R substituent, in good agreement with trends

(24) Shannon, R. D. *Acta Crystallogr.* **1976**, *A32*, 751−760
(25) Hammond, G. S. *J. Am. Chem. Soc.* **1955**, *77*, 334−338.

Table 6. Substituent Group Effects on the Cyclization Energy Barrier ($\Delta E^{\ddagger}$) and on Geometrical Parameters in the Cyclization Transition States for Hydroamination/Cyclization of $H_2N(CH_2)_3C{\equiv}C-R$ Substrate Mediated by the $Cp_2SmCH(TMS)_2$ Catalyst System[a]

	CH_3	H	Me_3Si
computed $\Delta E^{\ddagger}$ (kcal/mol)	8.8	5.1	4.9
experimental N_t[b]	96	580	7600
$Sm-Cp_{centroid}$	2.527	2.524	2.525
Sm−N1	2.325	2.322	2.340
Sm−C1	2.586	2.589	2.585
C1−C2	1.262	1.256	1.269
N1−C2	2.211	2.277	2.139
C1−C2−R	139.0	137.5	136.9

[a] Labeling refers to Figure 2. [b] Turnover frequency data (N_t h^{-1} at 21 °C) from ref 9b.

observed experimentally.[9b] Structural analysis of the transition states as a function of R substituent (Table 6) shows that the R moieties cause only slight geometrical distortions in the catalytic site environment. In particular, the bond lengths ($Sm-Cp_{centroid}$, Sm−N1, Sm−C1) associated with the coordinating groups remain nearly constant, while there are no significant changes of the C1−C2 multiple bond lengths nor of the C1−C2−R angles, both representing indicators of possible structural distortions induced by the R substituents. Therefore, for the considered cases, the size of the R group plays a marginal role in the kinetics of the process, and hence, steric interactions can be considered of little relevance.

To understand how electronic contributions influence the kinetics of the aminoalkyne hydroamination/cyclization process, the charge distribution in the transition state has been analyzed. Experimental results[9b] implicate a seven-membered transition state, with a partial positive charge localized on metal and β carbon atoms and a negative charge localized on nitrogen and α carbon atoms (**E**).

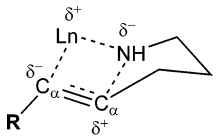

E

An NBO population analysis of cyclization transition states was performed to understand the substituent effects on the charge distribution. The computed values of the charges on the key atoms involved in the cyclization step show that the principal effects of the substituents involve alteration of the charge localized on the α carbon appended to the R group.

Note that the negative charge density on the α carbon increases substantially on proceeding from R = CH_3, to R = H, to R = trimethylsilyl. The increased electron density enhances the interaction between the electrophilic lanthanide center and the α carbon, thus stabilizing the transition state. The effect of methyl and the $SiMe_3$ substituent groups on the charge distribution in the transition state has been noted previously.[26] The observed computational trends find close parallels in the kinetic experimental data.[9a,b]

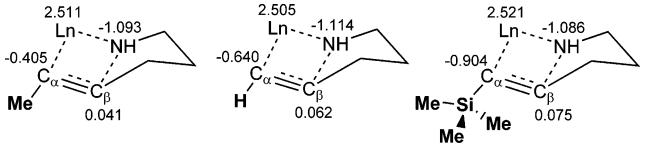

Concluding Remarks

Catalyst generation and aminoalkyne hydroamination/cyclization processes at an electrophilic Cp_2Sm- site have been investigated using DFT and analytical gradient methods to understand catalytic reaction pathways and accompanying reaction energetics. It is found that the process consists of two discrete steps, namely, cyclization and protonolysis, superficially similar to the parent aminoalkene hydroamination. Nevertheless, the cyclization step is computed to be thermoneutral in the case of aminoalkenes, while it is significantly exothermic for aminoalkynes, as found experimentally. From computed activation energetics, the alkyne insertion process represents the turnover-limiting step, followed by a rapid and irreversible protonolysis step, in agreement with experiment. Lanthanide and substituent effects on the reaction rate have also been investigated. Cyclization rates are found to increase upon decreasing the size of the catalyst lanthanide center, in excellent agreement with experiment. $RC{\equiv}C-$ substituents on aminoalkyne substrates accelerate cyclization rates via the electron density buildup on the adjacent C atom, also in excellent agreement with experiment.

Acknowledgment. This research was supported by the Ministero dell'Istruzione, dell'Università e della Ricerca (MIUR Rome), the Consiglio Nazionale delle Ricerche (CNR Rome), and by the U.S. National Science Foundation (grant CHE-04157407).

Supporting Information Available: Complete list of Cartesian coordinates for all structures and data from the IRC calculations presently analyzed. This material is available free of charge via the Internet at http://pubs.acs.org.

OM060717G

(26) (a) Horton, A. D. *Organometallics* **1991**, *10*, 3910−3918. (b) Burger, B. J.; Thompson, M. E.; Cotter, W. D.; Bercaw, J. E. *J. Am. Chem. Soc.* **1990**, *77*, 1566−1577.